Carbonates Evaporites (2018) 33:223–234
https://doi.org/10.1007/s13146-017-0333-x

ORIGINAL ARTICLE

Using stable isotopes and major ions to identify hydrogeochemical characteristics of karst groundwater in Xide country, Sichuan Province

Jianfei Yuan[1] · Fen Xu[2] · Guoshi Deng[1] · Yeqi Tang[1]

Accepted: 24 January 2017 / Published online: 14 February 2017

Abstract Karst groundwater is important water resources for local people in southwest China, especially in Xide country, Sichuan Province. Stable isotopes (H and O) that incorporated with major ions of groundwater were used to identify the origin of groundwater, and determine the dominant water–rock interaction processes controlling the hydrogeochemical characteristics of groundwater in the study area. The stable isotopes results indicated that all groundwater derived from meteoric water. The chemical analysis showed that the cold groundwater was HCO_3-Ca·Mg type, and the thermal water was HCO_3·SO_4-Ca·Mg type. The major ions of groundwater combined with the equilibrium stated of the groundwater based on the saturation index (SI), suggested that the hydrogeochemical characteristic of groundwater was mainly governed by dissolution of carbonate minerals and gypsum rocks, and ion exchange. Other factors such as evaporation and anthropogenic activities may also play roles on it. The results revealed the dominant hydrogeochemical processes controlling groundwater water quality in this karst area, which would provide significant insights into the local governments that can make effective policy for groundwater utilization.

✉ Jianfei Yuan
jianfeiyuan@163.com

[1] Chengdu Center, China Geological Survey, Chengdu 610081, Sichuan, People's Republic of China

[2] School of Environmental Studies, China University of Geosciences, Wuhan 430074, Hubei, People's Republic of China

Keywords Oxygen and hydrogen isotope · Major ions · Water–rock interactions · Karst groundwater · Xide country · Sichuan Province

Introduction

Southwest China is one of the largest karst areas in the world (covers about 780,000 km^2) where karst groundwater is a vital source of drinking water to about 100 million people (Cai 1996; Jiang et al. 2006; Peng et al. 2011). Karst groundwater in these areas can be divided into two systems, including the covered-buried karst water system and the bare karst water system. The main strata in these areas include Devonian, Permian, and Lower and Middle Triassic, which typically develop from carbonate rocks (Jiang et al. 2006). Being important resources of drinking water for southwest China, extensive studies have been studied in these karst areas, which were principally focusing on topography and geological structure, runoff respond to rainfall, hydrological dynamics of under-groundwater, and the influence of land cover on hydrogeochemistry, tracer test for tracing the connection of karst groundwater in karst aquifer (Chen et al. 2013; Hu et al. 2015; Jia et al. 2004; Lan et al. 2015; Liu et al. 2011, 2015; Pan et al. 2015; Sebela and Liu 2014; Zhao et al. 2015). However, seldom studies were conducted to the hydrogeochemical processes that control the quality and chemical component of karst groundwater in karst aquifer, especially in Xide country.

The hydrogeochemical processes taking place in karst aquifer are governed by many factors, such as the composition of rain water, geological structure and mineralogy of aquifer, and water–rock interaction along the flow paths (Alberto Sanchez–Sanchez et al. 2015; Delbart et al. 2016; Grimmeisen et al. 2016; Ma et al. 2011; Thilakerathne

et al. 2015; Wang et al. 2015a, b; Yang et al. 2010, 2013). Beyond that, karst groundwater systems are also vulnerable to anthropogenic activities, including excessive agricultural practices, chemical fertilizers, mining activities, and domestic sewage (Bhat et al. 2014; Calijuri et al. 2012; Han et al. 2013; Jiang et al. 2008; Lang et al. 2006; Re et al. 2014; Yuan et al. 2016). However, it is worth noting that karst aquifer is a unique and complex flow system due to high heterogeneity in geology and geomorphologic conditions, and special water–rock reactions, etc. (Han et al. 2014). Thus, it is difficult to identify the dominant hydrogeochemical processes that control the hydrogeochemical characteristics of groundwater by conventional hydrogeochemical studies.

Previous studies have demonstrated that spatial variations in the chemical characteristics of karst groundwater can be effective to interpret the origin of groundwater and water–rock interactions in aquifer (Han et al. 2013). In addition, stable isotopes (H and O) are useful tracers for recognizing the origin and pathways of groundwater recharge. Combined major ions and stable isotope in karst groundwater could help determine the karst groundwater origin, movement, and hydrogeochemical processes that contributed to hydrogeochemical characteristics (Pu et al. 2013; Wang et al. 2015b; Yuan 2013). However, few comprehensive works were carried on the hydrogeochemical processes in karstic aquifers by combing stable isotopes and major ions (Pu 2013; Pu et al. 2013; Yuan et al. 2016).

The study area, Xide country, is a Yi ethnic community in southwest Sichuan, located in southwest China. Several karst springs and thermal water occur along the Sunshui River are the dominant drinking and irrigation water resources for local people in the western part of Xide country. In spite of the importance of karst groundwater in these areas, the exploitation degree of groundwater in these karst areas is generally low, due to the complicated hydrogeologic conditions and the relatively backward regional economy. Understanding the hydrogeochemical processes occurring in these karst areas is, therefore, critically needed for the policy making of local governments in the light of karst groundwater utilization and management (Wang et al. 2006).

This study investigated the predominant hydrogeochemical processes that govern hydrogeochemical characteristics of karst groundwater in Xide country. The spatial variations of stable isotopes (O and H) and major ions in groundwater are applied to identify the origin of groundwater and determine the dominant hydrogeochemical processes that controlling the chemical compositions of karst groundwater. The results would provide a basis of developing strategies for water resources utilization in Xide country.

Geology and hydrogeology setting

The study area is situated in the Xide country of Sichuan province, southwest China. Its elevation ranges from 1580 to 3500 m above mean sea level, and shows a declining from north to south, and from east to west. A subtropical monsoon climate dominates here with an annual mean temperature of 14 °C. The annual precipitation is 1006 mm, and about 88% of its rain falls between May and October. The Sunshui River is the most important river in Xide country, with a total length of 110 km and an area of 1617.5 km^2. It flows through some rivers and streams, with an average discharge of 37.2 m^3/s.

Two main sets of faults are found to control the structure in this area (Zhao 1987). The first one is the set of NE–SW trending faults, which belong to the Anning River tectonic system. The second one is the set of NW–NS trending faults that crosswise distributing in the western part of Xide country. These faults with multi-period cut the stratum into various patterns of geological tectonic units with different lithologies. The outcrops in our study area are made up of carbonate rock, clastic rock and metamorphic rock from the Proterozoic system to Quaternary system except the Carboniferous system, Permian system, Silurian system and Cambrian system. As shown in Figs. 1 and 2, the exposed strata are principally sea platform carbonate rocks of Sinian strata, followed by earlier Triassic continental-facies clastic rocks. Sulfate evaporate strata, though minor, also exists in the region studied.

Dolomitic limestone is the predominant aquifer in the study area, from which cold and thermal springs emerged occasionally, with flow ranging from 0.50 to 284.00 L/s. The others are mainly clastic rocks, and the flow of springs distributed in those aquifers is lower than that of dolomitic limestone aquifer, which ranged from 0.09 to 0.15 L/s. In general, groundwater is ultimately discharged to the Sunshui River along the flow paths (from north and south).

Sampling and analysis

A total of twelve cold and thermal water samples were sampled from spring and borehole in August 2014. Groundwater temperature (T), electrical conductivity (EC), pH, and the total dissolved solid (TDS) were determined in situ by portable Hanna meters (HI991301). The free carbon dioxide (CO_2-free) was also measured in situ in term of standard methods (Yang et al. 2015). Alkalinity was measured within 12 h in terms of the Gran titration method. All groundwater samples were filtered through a 0.45 μm filter and stored in new 500 ml polyethylene bottles. Groundwater samples for cation measurement were

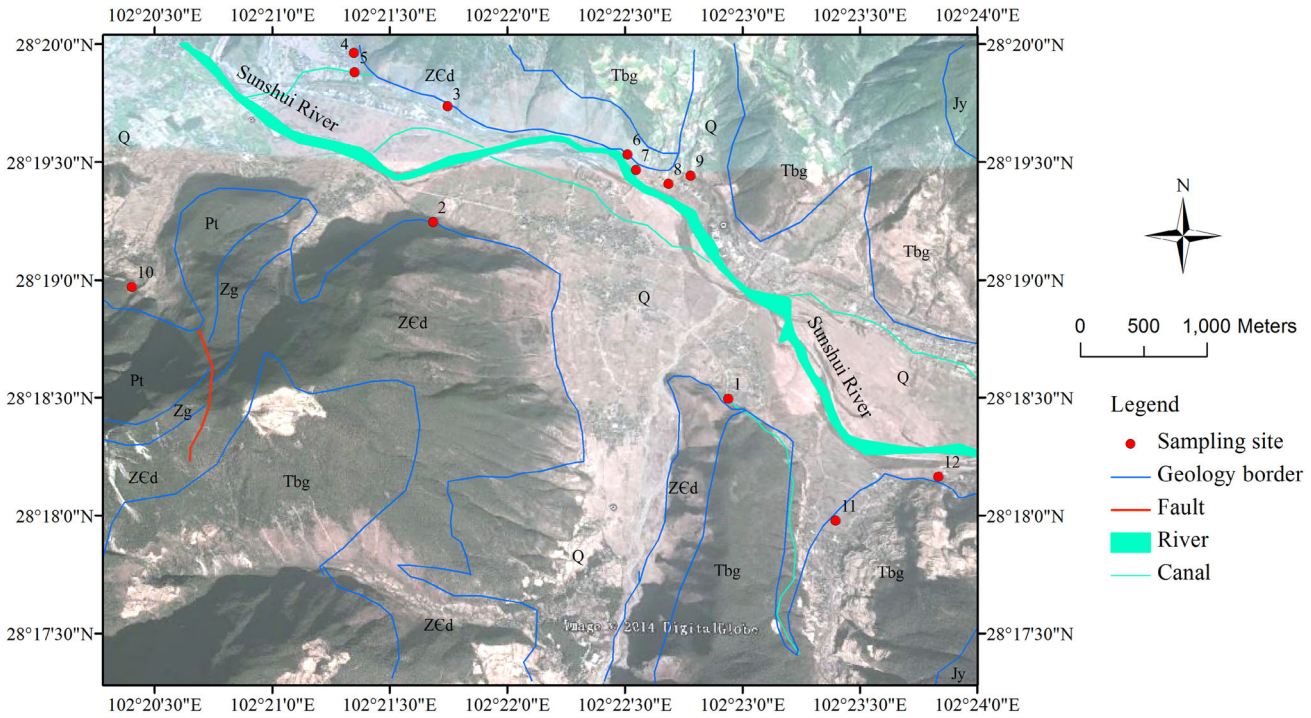

Fig. 1 The sketch geological map and sampling location of the study area

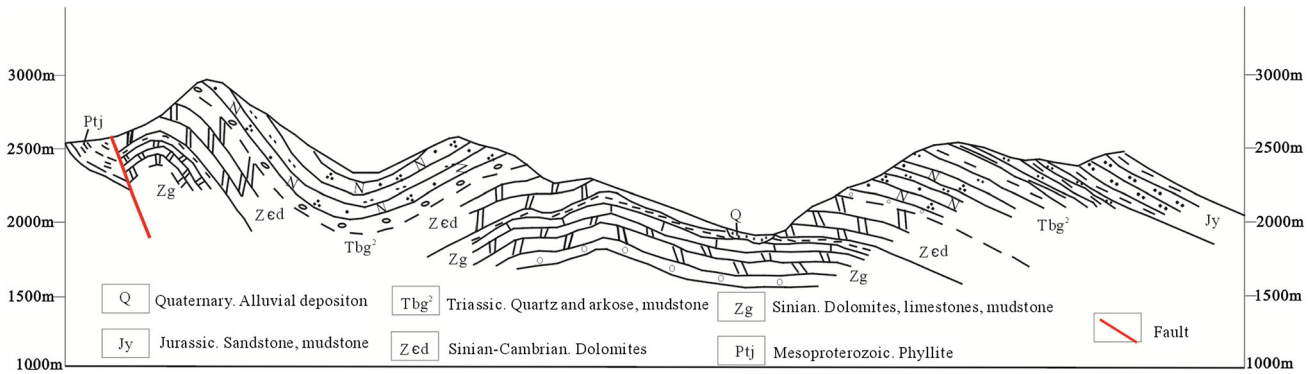

Fig. 2 Geological cross-section from northwest to southeast of our study area

acidified with ultrapure HNO_3 to pH < 2. Anions (Cl^-, and SO_4^{2-}) were measured using ion chromatography (IC, Dionex), and cations (Ca^{2+}, Mg^{2+}, Na^+, and K^+) were determined by inductively coupled plasma optical emission spectrometry (ICP-OES, Perkin Elmer Icap 6300). The charge balances and uncertainties of the measured cation and anion concentrations were within 5%.

Groundwater samples were also collected to measure the stable oxygen and hydrogen isotopes by mass spectrometer (MAT253) at the Institute of Karst Geology, Chinese Academy of Geological Science. The analytical precision of $\delta^{18}O$ and δD was 0.1 and 1‰, respectively. The former was determined by the CO_2 equilibration method and the latter was by the Zn reduction method (Coleman et al. 1982).

The saturation index (SI) of major minerals, including calcite ($SI_{Calcite}$), dolomite ($SI_{Dolomite}$), gypsum (SI_{Gypsum}) and anhydrite ($SI_{Anhydrite}$), was calculated to estimate the chemical equilibrium between groundwater and minerals by the geochemical program PHREEQC (Parkhurst and Appelo 1999).

Results and discussion

Oxygen and hydrogen isotopes

As shown in Fig. 3, almost all thermal and cold groundwater were distributed around the Global Meteoric Water Line (GMWL) (solid line: $\delta D = 8\delta^{18}O + 10$) (Craig

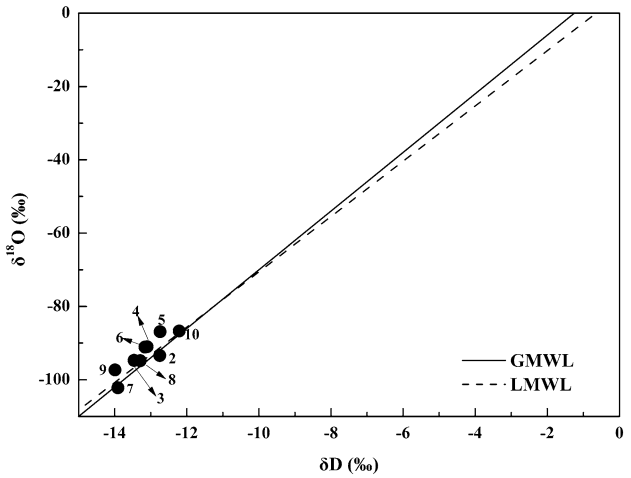

Fig. 3 Variation of $\delta^{18}O$ and δD in groundwater associated with GMWL and LMW

1961) and Local Meteoric Water Line (LMWL) (dash line: $\delta D = 7.54\delta^{18}O + 4.84$) (Liu et al. 1997). The δD and $\delta^{18}O$ values of thermal water ranged from −94.8 to −102.2‰ and −13.29 to −13.99‰, respectively, while that of cold groundwater varied from −86.9 to −94.7‰ and −12.74 to −13.46‰, respectively. There was no obvious isotope shift in $\delta^{18}O$ values for thermal and cold groundwater, indicating that all water samples were meteoric origin. Moreover, it is worth mentioning that the cold groundwater samples were relatively enriched in heavier isotopes than those of thermal water samples, which may be explained as the results of the different recharge altitude and geological conditions. Previous studies have demonstrated that the altitude effectiveness of isotope could be used to calculate the recharge altitude of groundwater, and then reveal the recharge area (Krimisssa et al. 1994; Yuan 2013; Zhou et al. 2015). The calculation results showed that the recharge altitude of thermal water ranged from 2874 to 3092 m, while that of cold groundwater was about 2584–2818 m. In addition, the elevation of mountain situated in the north of the Sunshui River ranged from 2400 to 3300 m, which may be the dominant recharge area for the thermal water samples located in the north of the Sunshui River. The difference in recharge altitude could lead to heavier isotopes enrich in cold groundwater with lower recharge altitude. Furthermore, the thermal water samples derived from the deep circulation groundwater, which was controlled by fracture. The recharged cold groundwater flowed through fracture to form thermal water, and then reached the surface. While the cold spring samples originated from shallow cycle dissolved-fissure type groundwater. The precipitation from low recharge altitude transported along the dissolved-fissure or sinkholes, and then outcropped near river valley, formed cold spring. Thus, the difference in geological conditions for thermal water and cold groundwater formed could also result in the enrichment of heavier isotopes in cold groundwater.

Hydrogeochemisty of cold and thermal groundwater

The pH of cold groundwater (except for No. 6) ranged from 7.01 to 7.62, was slightly higher than that of thermal groundwater, which was 6.68–6.95. The lower pH occurred in thermal groundwater may be because the thermal water was derived from the deep circulation groundwater, more CO_2-free was generated through the dissolution of deep-carbonate minerals at high temperature (Table 1), and thus leading to the lower pH in thermal groundwater. It agreed with the concentration of CO_2-free in thermal and cold groundwater. As shown in Table 1, the concentration of CO_2-free in thermal groundwater varied from 92.4 to 165 mg/L, while that in cold groundwater ranged from 5.5 to 70.4 mg/L, with an average of 18.7 mg/L. The TDS was variable in different aquifers. It ranged from 102.1 to 847.4 mg/L in dolomitic limestone aquifer (Table 1), while it was of 51.8 mg/L and 85.9-142.4 mg/L in metamorphic terrain and clastic sediment aquifer, respectively. This may be associated with the mineralization of major minerals in the aquifers, and was demonstrated in the next section. Furthermore, The TDS of thermal groundwater samples were general higher than that of cold groundwater, suggesting stronger water–rock interaction occurring at high temperature.

The mean concentrations of HCO_3^-, SO_4^{2-}, and Cl^- in thermal water were of 474.0, 190.2, and 61.0 mg/L, which were higher than that of cold groundwater. In addition, the dominant cation was Ca^{2+}, followed by Mg^{2+} in all aquifers. Piper diagram showed that most of the cold groundwater from the dolomitic limestone aquifer and clastic sediment aquifer were predominantly of HCO_3-Ca·Mg types, while that of thermal water was of HCO_3-SO_4-Ca·Mg type (Fig. 4). The dominance of (Ca^{2+} + -Mg^{2+}), together with HCO_3^- maybe result from the dissolution of carbonate minerals (dolomitic and calcite) and gypsum rocks in the study area.

Geochemical evolution of groundwater

The geochemical evolution of groundwater is mainly controlled by atmospheric precipitation, water–rock interaction and evaporation (Krimisssa et al. 1994; Wang et al. 2006; Yuan 2013). In this study, the Gibbs diagram was introduced to distinguish the dominant processes that controlling the hydrogeochemical characteristic of groundwater. It contains three distinct segments, including atmospheric precipitation dominance, rock dominants and evaporation dominance (Gibbs 1970). As shown in Fig. 5,

Table 1 Physical and chemical parameters of water samples in the study area (in mg/L, except for T in °C, EC in μs/cm, δD and $\delta^{18}O$ in ‰, and "-" not measured)

No	Types	Locality	Aquifer	Sampling data	Longitude	Latitude	Altitude (m)	Q (L/s)	T	EC
1	Groundwater	Xincun village	Dolomite	8/14/2014	102°22′56.5″	28°18′29.7″	1828	11.40	15.0	136.9
2	Groundwater	Xingfu village	Dolomite	8/14/2014	102°21′41.0″	28°19′14.7″	1798	2840.00	13.4	140.0
3	Groundwater	Yuanquan village	Dolomite	8/14/2014	102°21′44.8″	28°19′44.1″	1778	1000.00	11.5	160.2
4	Groundwater	Yuanquan village	Dolomite	8/14/2014	102°21′20.9″	28°19′57.8″	1815	18.25	12.8	187.6
5	Groundwater	Yuanquan village	Dolomite	8/14/2014	102°21′21.1″	28°19′52.8″	1804	12.51	14.0	222.1
6	Groundwater	Xingfu village	Dolomite	8/14/2014	102°22′30.8″	28°19′31.9″	1811	32.40	21.0	430.0
7	Thermal water	Xingfu village	Dolomite	8/15/2014	102°22′32.9″	28°19′27.9″	1802	11.30	42.0	1130.0
8	Thermal water	Xingfu village	Dolomite	8/15/2014	102°22′41.2″	28°19′24.3″	1831	0.50	45.0	917.0
9	Thermal water	Xingfu village	Dolomite	8/15/2014	102°22′46.9″	28°19′26.4″	1791	5.76	62.0	1187.0
10	Groundwater	Sihe village	Metamorphic rock	8/14/2014	102°20′24.2″	28°18′58.1″	2060	0.91	13.2	64.5
11	Groundwater	Shaluo village	Clastic rock	8/14/2014	102°23′23.9″	28°17′58.6″	1859	0.09	14.2	155.0
12	Groundwater	Shaluo village	Clastic rock	8/14/2014	102°23′50.0″	28°18′09.8″	1836	0.15	15.0	220.0

No	pH	Na^+	K^+	Ca^{2+}	Mg^{2+}	Cl^-	SO_4^{2-}	HCO_3^-	CO_2-free	TDS	Water type	$SI_{Calcite}$	$SI_{Dolomite}$	SI_{Gypsum}	$SI_{Anhydrite}$
1	7.01	4.1	4.4	21.9	7.9	20.0	13.3	71.6	13.2	128.9	HCO_3·Cl–Ca·Mg	−1.17	−2.44	−2.80	−3.10
2	7.38	0.9	1.2	24.3	12.1	7.1	6.7	120.3	12.1	120.9	HCO_3–Ca·Mg	−0.55	−1.04	−3.08	−3.38
3	7.15	0.6	0.7	20.9	11.2	6.0	5.3	106.1	17.6	102.1	HCO_3–Ca·Mg	−0.88	−1.69	−3.23	−3.53
4	7.18	7.4	1.3	21.8	12.3	7.9	22.0	109.7	14.3	132.6	HCO_3–Ca·Mg	−0.84	−1.58	−2.61	−2.92
5	7.62	6.5	1.3	29.3	16.3	11.9	19.9	141.5	6.6	162.3	HCO_3–Ca·Mg	−0.18	−0.27	−2.57	−2.87
6	6.65	20.1	10.5	58.6	25.2	47.6	80.1	187.5	70.4	351.2	HCO_3·SO_4–Ca·Mg	−0.80	−1.61	−1.78	−2.09
7	6.68	51.4	25.6	131.9	64.3	127.0	203.1	424.5	165	847.4	HCO_3·SO_4–Ca·Mg	−0.17	−0.32	−1.24	−1.54
8	6.95	33.4	22.9	115.0	46.5	24.3	162.5	467.0	105.6	647.7	HCO_3·SO_4–Ca·Mg	0.10	0.16	−1.34	−1.64
9	6.94	45.4	28.4	129.4	56.6	31.7	205.0	530.6	92.4	815.1	HCO_3·SO_4–Ca·Mg	0.18	0.33	−1.23	−1.53
10	7.04	5.8	1.0	5.5	3.1	2.8	13.7	28.3	5.5	51.8	HCO_3·SO_4–Ca·Mg·Na	−2.28	−4.62	−3.28	−3.71
11	7.25	3.0	1.7	18.2	4.4	6.0	5.6	70.7	8.8	85.9	HCO_3–Ca·Mg	−1.00	−2.27	−3.21	−3.52
12	7.25	5.0	1.3	29.6	9.4	4.0	4.6	141.5	19.8	142.4	HCO_3–Ca·Mg	−0.52	−1.19	−3.16	−3.46

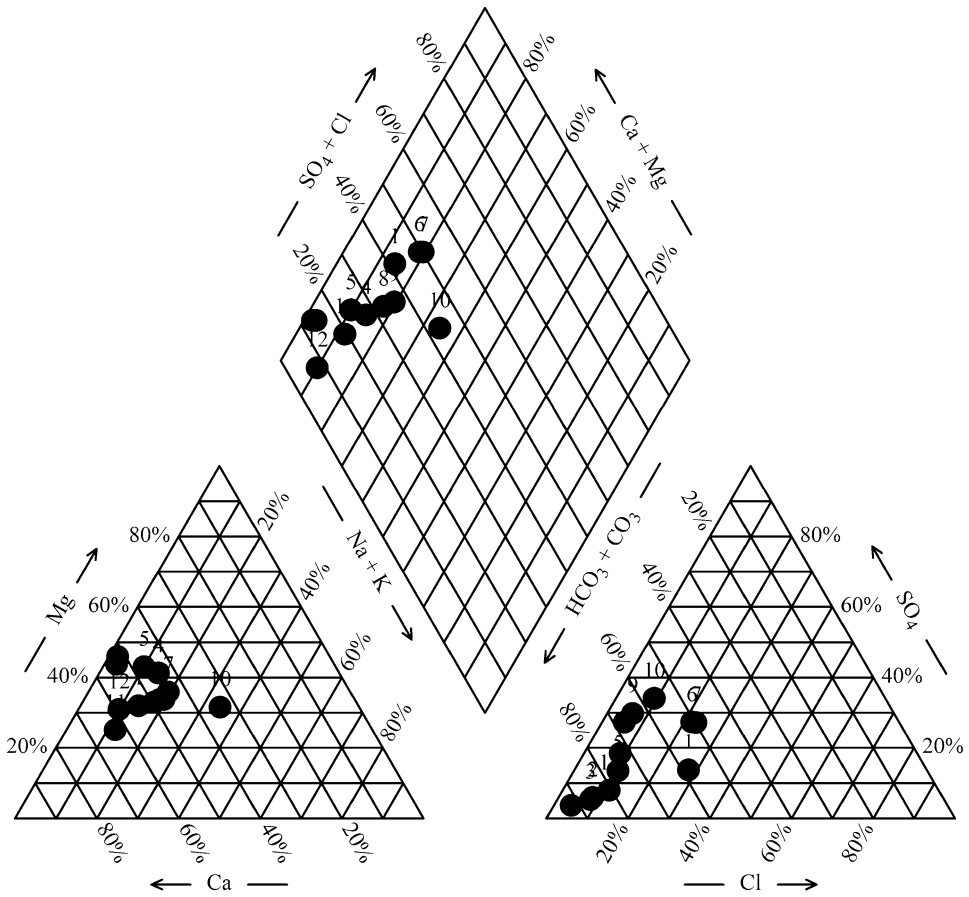

Fig. 4 Piper diagram of cold and thermal groundwater samples in the study area

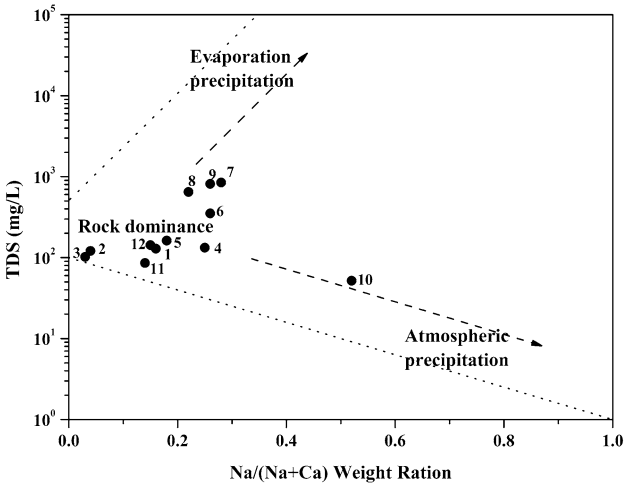

Fig. 5 Plot of Na/(Na + Ca) weight ration vs. TDS of groundwater collected from the study area

both thermal water and cold groundwater (except for sample 10) scattered in rock dominance segment, implying that water–rock interaction was the predominant hydrogeochemical processes that regulated the chemical components of groundwater. It was worth noting that sample 10 plotted closely to atmospheric precipitation dominance segment, meaning that the chemical component of sample 10 was affected by atmospheric precipitation. Moreover, the TDS of sample 10 was relatively lower than other samples. This may be due to that sample 10 was collected from a higher altitude metamorphic aquifer (Table 1), which had a shorter flow path, and then resulting in a weak water–rock interaction.

Saturation index (SI)

SI is useful to illustrate the water–rock interaction in karst aquifer system. Generally, the minerals were saturated or supersaturated in groundwater as the SI of minerals are greater than 0. On the contrary, if SI value is less than 0, the major minerals were under-saturated with groundwater. In the study area, SI of carbonate minerals (Calcite and Dolomite) for thermal water (No. 7 and No. 8) were greater than 0 (Table 1), meaning that thermal groundwater was saturated or supersaturated with carbonate minerals. However, SI was less than 0 for all cold groundwater. This could be because thermal water is conducive to the dissolution of carbonate minerals, and/or thermal groundwater stem from deep circulation groundwater, which had experienced prolonged residence time with these minerals than

cold water, and therefore, leading to more carbonate minerals dissolved. Additionally, both thermal and cold groundwater were unsaturated with gypsum and anhydrite minerals, suggesting that the water–rock interaction in the karst aquifer did not reach equilibrium, and more gypsum and anhydrite could be dissolved in groundwater. This could be considered as insufficient gypsum and anhydrite minerals sources in this study area, and consequently resulted in limited interactions between groundwater and minerals (Han et al. 2013).

Furthermore, diagram analyses of TDS, SI and major ions were employed to illustrate the origin of chemical constituents of karst groundwater (Han et al. 2013). The results can be used to identify dominant hydrological processes in this study area.

There was obvious correlation between the concentrations of major ions (Ca^{2+}, Mg^{2+} and HCO_3^-) and $SI_{Calcite}$ (Fig. 6a) and $SI_{Dolomite}$ (Fig. 6b) for most groundwater except thermal groundwater, implying that more calcite and dolomite could be dissolved in cold groundwater along groundwater flow path. Moreover, there were distinct differences in hydrogeochemical characteristics of groundwater collected from different aquifers. This could be the result of the flow at different aquifers were variable, causing different residence time, and thus affected the interaction between groundwater and reservoir minerals. In addition, SI_{Gypsum} of all groundwater samples were less than 0, and was positively associated with Ca^{2+}, SO_4^{2-} and TDS (Fig. 6c and Fig. 6d), implying that more gypsum minerals can be dissolved along the groundwater flow direction, which then can release more Ca^{2+} to groundwater. Furthermore, there was also obvious positive relationship between the concentration of Ca^{2+}, Mg^{2+}, HCO_3^- and SO_4^{2-} vs. TDS (Fig. 6e, f), respectively. For cations, the slope between Ca^{2+} and TDS ($r^2 = 0.992$) was much greater than those for K^+, Na^+ and Mg^{2+} (Fig. 6e), meaning that the concentration of Ca^{2+} made the biggest contribution to TDS in groundwater than other cations. And for anions, the concentration of HCO_3^- and TDS showed the highest slop than Cl^- and SO_4^{2-} (Fig. 6f). The results were consistent with hydrochemical types of groundwater in this area (Fig. 4).

Primary reactants dissolution in the study area

It has been well demonstrated that the variation of chemical compositions of groundwater can be applied to illustrate the hydrogeochemical processes that is taking place in the karst aquifers (Yuan et al. 2016). In Xide country, karst aquifers are mainly made up of dolomite and dolomitic limestone of Sinian. Generally, the dissolution of calcite and dolomite released Ca^{2+} and Mg^{2+}, and thus lead to high concentration of Ca^{2+} and Mg^{2+} in karst groundwater (Han et al. 2014). It was assumed that calcite was the sole source of Ca^{2+} in groundwater of our study area. When it dissolved, released Ca^{2+} and HCO_3^- into groundwater, and therefore the slope of $[Ca^{2+}]/[HCO_3^-]$ would be 1:1–1:2, as following:

$$CaCO_3 + H^+ = Ca^{2+} + HCO_3^- \quad (1)$$

$$CaCO_3 + H_2O + CO_2 = Ca^{2+} + 2HCO_3^- \quad (2)$$

As shown in Fig. 7a, the concentration of Ca^{2+} increased with increasing HCO_3^-, and there was a good linear relationship between them (Fig. 7a). Additionally, the concentration of HCO_3^- increased as TDS increased (Fig. 6f), and $SI_{Calcite}$ is less than 0 for cold groundwater (Fig. 6a), implying that calcite dissolution is a feasible source of Ca^{2+} and HCO_3^- for cold groundwater in the study area. While the slope of $[Ca^{2+}]/[HCO_3^-]$ was less than 1:2. The low $[Ca^{2+}]/[HCO_3^-]$ ratios could be the result of either an extract source of HCO_3^- or Ca^{2+} depletion by cation exchange change. Likewise, the total concentration of Ca^{2+} and Mg^{2+} increased with increasing HCO_3^- (Fig. 7b), meaning that dolomite should be another source of Ca^{2+} and HCO_3^-. Previous studies suggested that if the mole ratio of $([Ca^{2+}] + [Mg^{2+}]):[HCO_3^-]$ is 1:1 to 1:2, the dissolution of calcite and dolomite, not distinguish, may main sources of Ca^{2+} and Mg^{2+} in groundwater (Bhardwaj et al. 2009). In the study area, the $([Ca^{2+}] + [Mg^{2+}]):[HCO_3^-]$ of cold and thermal groundwater from karst aquifer, metamorphic aquifer and clastic rock aquifer were between 0.5 and 1.0, indicated that the carbonate rocks were the main source of Ca^{2+}. Moreover, thermal groundwater and sample No. 6 were slightly deviated from the lines of $[Ca^{2+}]:[HCO_3^-]=1:2$ and $([Ca^{2+}]+[Mg^{2+}]):[HCO_3^-]=1:2$, implying that there was other likely source of $[Ca^{2+}]$, such as gypsum dissolution.

When gypsum dissolution, the ration of $[Ca^{2+}]/[SO_4^{2-}]$ would be 1:1 (Wang et al. 2006). As shown in Fig. 7c, Ca^{2+} was positively correlated with SO_4^{2-}, and the ratio $[Ca^{2+}]:[SO_4^{2-}]$ was 1.380. It meant that the dissolution of gypsum was a source of Ca^{2+} and SO_4^{2-} for groundwater in the study area, and the higher ratio of $[Ca^{2+}]:[SO_4^{2-}]$ may be results of dissolution of carbonate as well as gypsum. Beyond that, ion exchange may also be an important source of Ca^{2+} in thermal and cold groundwater.

Ion exchange and possible source of sodium

Though Na^+ and Cl^- were not the dominant ions in groundwater, the sources of them could also be used to identify the hydrogeochemical processes taking place in the aquifer. Previous study has demonstrated that halite sporadically distributed in our study area (Zhao 1987). The dissolution of halite may be a probable source of Na^+ and Cl^-. Generally, the relationship between Na^+ and Cl^- in

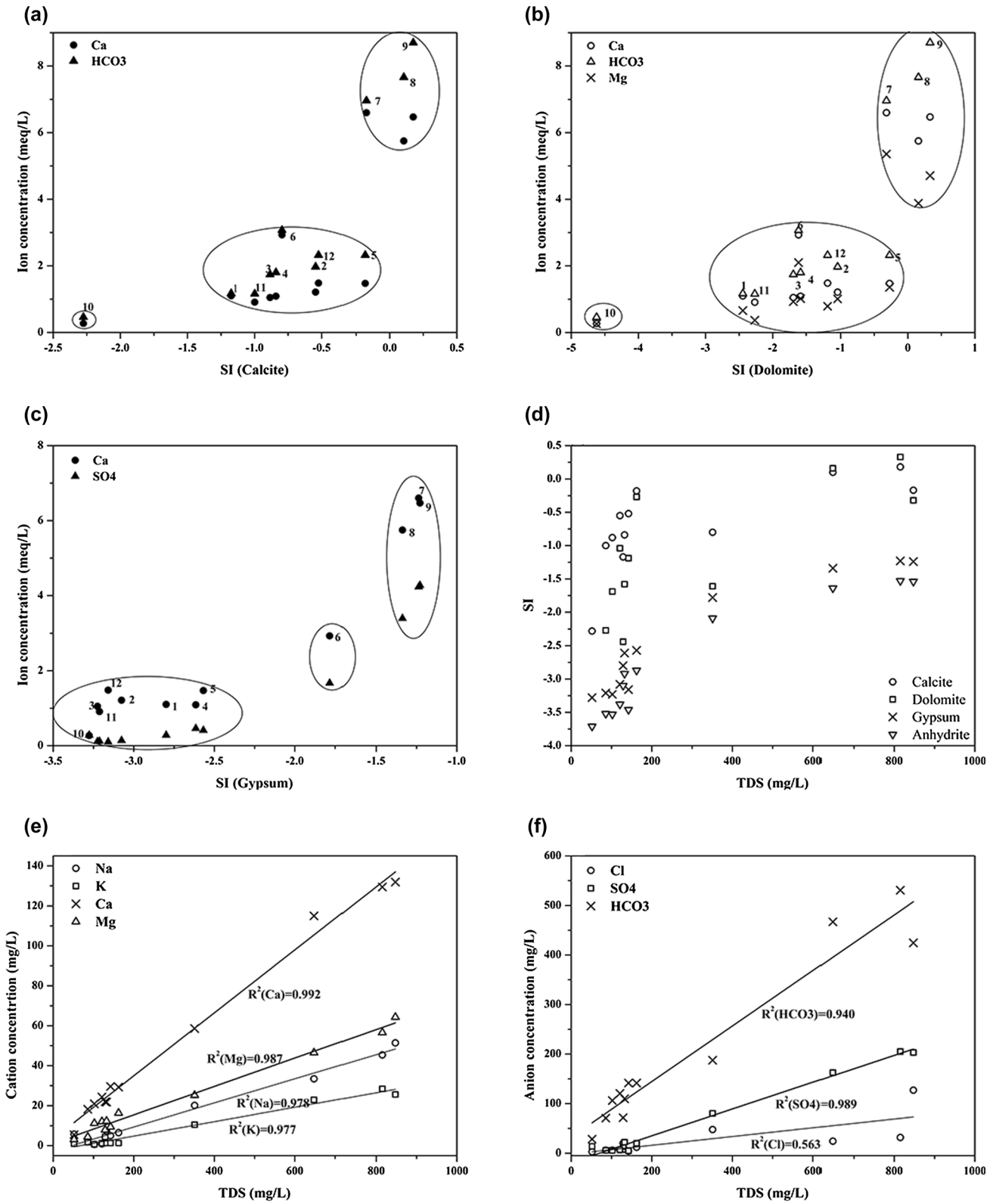

Fig. 6 *Plot* of $SI_{Calcite}$ (**a**), $SI_{Dolomite}$ (**b**), SI_{Gypsum} (**c**) vs. ion concentration, and SI values (**d**), cation concentration (**e**), anion concentration (**f**) vs. TDS

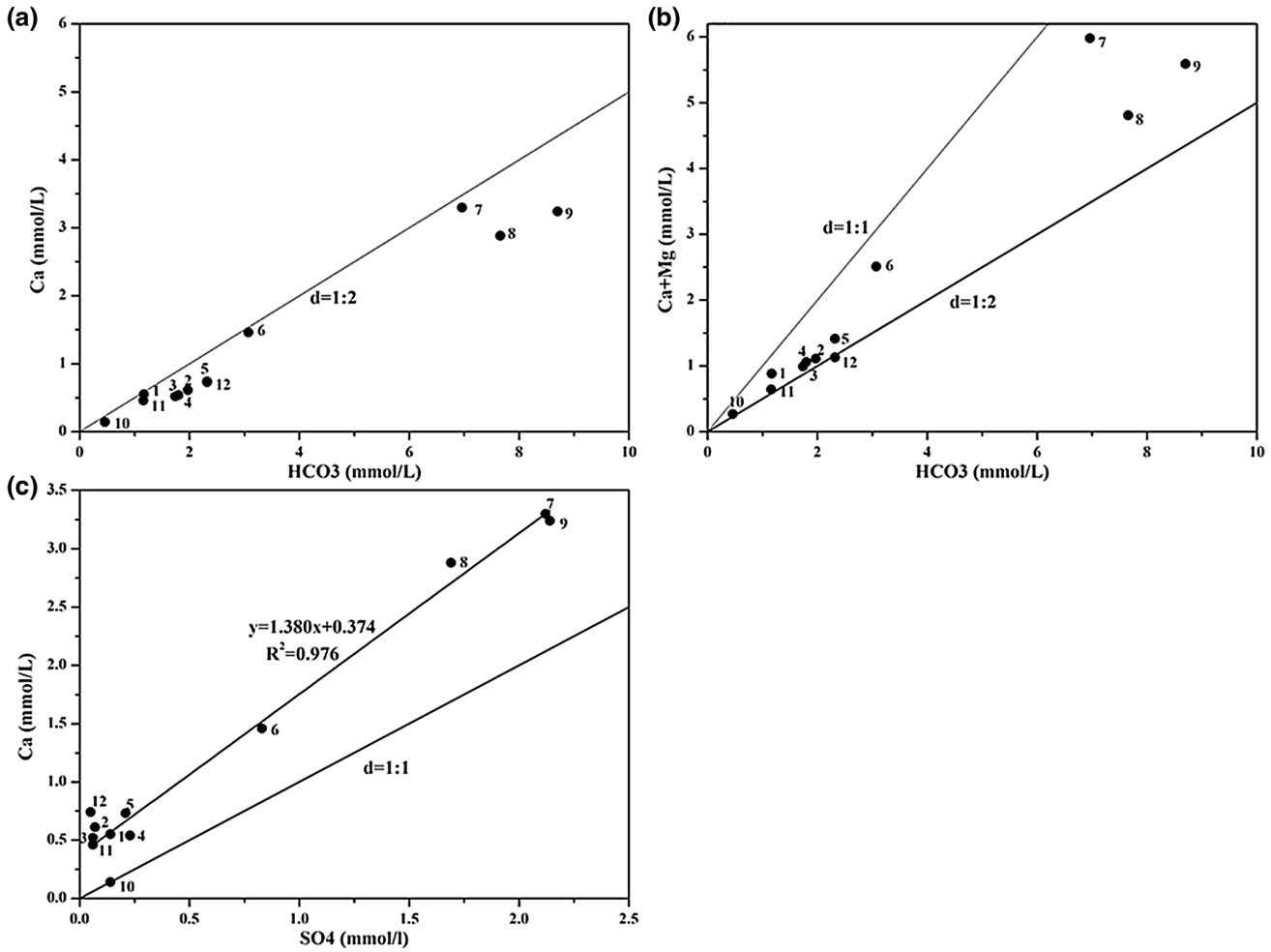

Fig. 7 *Plot* of the linear relationship of Ca (**a**), (Ca + Mg) (**b**) vs. HCO_3, and SO_4 vs. Ca (**c**)

groundwater can be used to interpret the source of Na^+ and Cl^-. If Na^+ and Cl^- mainly resulted from halite dissolution, the ration of Na/Cl would be a constant of 1.0. However, as shown in Fig. 8a, most of groundwater samples deviated from the line of Na and Cl (1:1), and the concentration of Na^+ and Cl^- was not high in groundwater (Table 1), thus it could conclude that the dissolution of halite was not an important source of Na^+ and Cl^-. Moreover, as mentioned above, Ca^{2+}, Mg^{2+}, $SO_4{}^{2-}$, and $HCO_3{}^-$ were dominant ions in groundwater, mainly originated from the dissolution of carbonate and gypsum. While, some groundwater samples plotted below or above the line of (Ca + Mg) and (SO_4 + HCO_3) (1:1), indicated that (Ca + Mg) was deficient or excess in these groundwater samples. On the contrary, Na^+ was excess or deficient in groundwater. The results signified that ion exchange could take place in the aquifer, which can be expressed as following formulation:

$$Ca^{2+}\left(\text{and/or } Mg^{2+}\right) + 2Na - EX = 2Na^+ + Ca\left(\text{and/or } Mg^{2+}\right) - EX \quad (1)$$

When ion exchange occurred in aquifer, Na^+ can be exchanged from minerals by Ca^{2+} or Mg^{2+} in groundwater, and therefore, leading to the concentration of Na^+ in groundwater increased, and instead, the concentration of Ca^{2+} or Mg^{2+} decreased. In Fig. 8c, the groundwater samples distributed in the right quadrant of the plot suggested that there was ion exchange in those groundwater samples. On the contrary, the samples located in the upper left quadrant of the diagram implied the presence of reverse ion exchange. It is worth noting that the concentrations of Cl in most water samples increased with a narrow variation ration of Na/Cl (less than 1) (Fig. 8d), which may be caused by evaporation and/or anthropogenic activities (Yuan et al. 2016). More works are needed to provide evidence in the future.

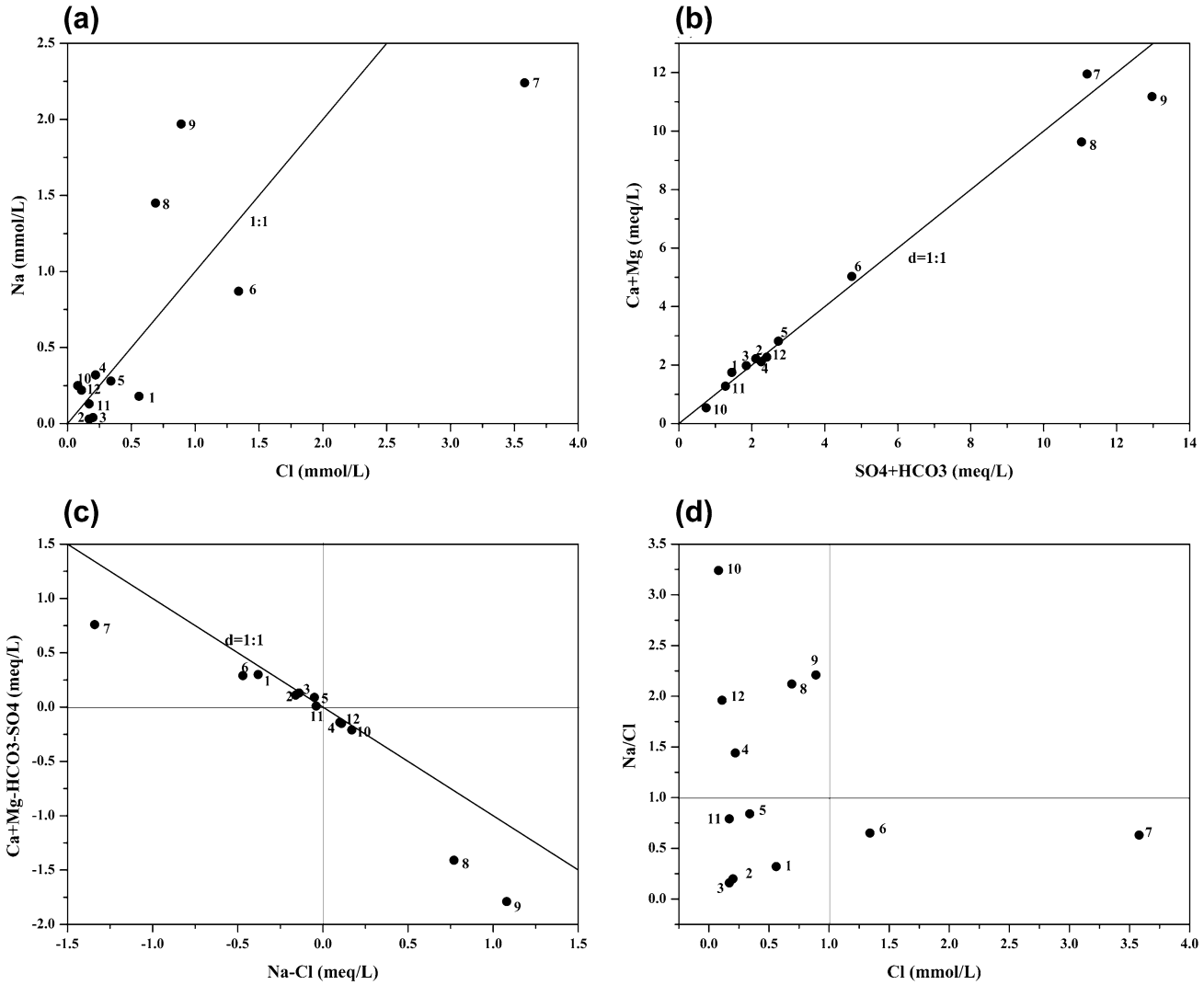

Fig. 8 *Plot* of Cl vs. Na (**a**), and (SO_4 + HCO_3) vs. (Ca + Mg) (**b**), (Na–Cl) vs. (Ca + Mg-SO_4–HCO_3). (**c**), and Cl vs. ration of Na and Cl (**d**)

Conclusions

Major ions that incorporated stable isotope ($\delta^{18}O$ and δD) were employed to identify the predominant hydrogeochemical processes that govern hydrogeochemical characteristics of karst groundwater in Xide country, Sichuan Province.

The results of stable isotope ($\delta^{18}O$ and δD) showed that both thermal and cold groundwater samples were of meteoric origin. Furthermore, cold groundwater was relatively enriched with heavier isotopes than thermal water. This may be due to the different recharge altitude and geological conditions of them. The chemical compositions of the groundwater were mainly governed by the water–rock interactions taking place in the aquifer. Ca^{2+}, Mg^{2+}, HCO_3^- and SO_4^{2-} were the major ions in groundwater in this study area. The cold groundwater was predominantly of HCO_3-Ca·Mg type, while the thermal water was mainly HCO_3·SO_4-Ca·Mg type.

The results of SI showed that both thermal and cold groundwater were unsaturated with gypsum and anhydrite minerals. In addition, calcite and dolomite were undersaturated in cold groundwater, while that for thermal water were saturated or supersaturated. The major ions of groundwater combining with equilibrium stated of the groundwater based on the SI indicated that the dissolution of carbonate rock (calcite and dolomite) and gypsum rock, and ion exchange were the dominant factors controlling hydrogeochemical characteristic of groundwater. Additionally, evaporation and anthropogenic activities may also play roles on the hydrogeochemical characteristics of groundwater.

Acknowledgements This research was financially supported by the China Geological Survey (No. 12120114030301) and the National Natural Science Foundation of China (No. 41502245). The authors would like to thank two anonymous reviewers who greatly improved the quality of the manuscript.

References

Alberto Sanchez-Sanchez J, Alvarez-Legorreta T, Pacheco-Avila JG, Gonzalez-Herrera RA, Carrillo-Bribiezca L (2015) Hydrogeochemical characterization of groundwater in the southern part of Quintana Roo, Mexico. Revista Mexicana De Ciencias Geologicas 32:62–76

Bhardwaj V, Singh DS, Singh AK (2009) Hydrogeochemistry of groundwater and anthropogenic control over dolomitization reactions in alluvial sediments of the Deoria district: Ganga plain, India. Environ Earth Sci 59:1099–1109

Bhat NA, Jeelani G, Bhat MY (2014) Hydrogeochemical assessment of groundwater in karst environments, Bringi watershed, Kashmir Himalayas, India. Curr Sci 106:1000–1007

Cai Y (1996) Preliminary research on ecological reconstruction in karst mountain poverty areas of southwest China. Adv Earth Sci 11:602–606 **(in Chinese with English abstract)**

Calijuri ML, do Couto DEA, Santiago DAF, Camargo DRA, e Silva MDFM (2012) Evaluation of the influence of natural and antrhopogenic processes on water quality in Karstic Region. Water Air Soil Pollut 223:2157–2168

Chen X, Zhang Y, Zhou Y, Zhang Z (2013) Analysis of hydrogeological parameters and numerical modeling groundwater in a karst watershed, southwest China. Carbonates Evaporites 28:89–94

Coleman ML, Shepherd TJ, Durham JJ, Rouse JE, Moore GR (1982) Reduction of water with zinc for hydrogen isotope analysis. Anal Chem 54:993–995

Craig H (1961) Isotopic variations in meteoric waters. Science 133:1702–1703

Delbart C, Valdés D, Barbecot F, Tognelli A, Couchoux L (2016) Spatial organization of the impulse response in a karst aquifer. J Hydrol 537:18–26

Gibbs RJ (1970) Mechanisms controlling world water chemistry. Science 170:1088–1090

Grimmeisen F, Zemann M, Goeppert N, Goldscheider N (2016) Weekly variations of discharge and groundwater quality caused by intermittent water supply in an urbanized karst catchment. J Hydrol 537:157–170

Han Y, Wang G, Cravotta CA III, Hu W, Bian Y, Zhang Z, Liu Y (2013) Hydrogeochemical evolution of Ordovician limestone groundwater in Yanzhou, North China. Hydrol Process 27:2247–2257

Han Z, Tang C, Wu P, Zhang R, Zhang C (2014) Using stable isotopes and major ions to identify hydrological processes and geochemical characteristics in a typical karstic basin, Guizhou, southwest China. Isot Environ Health Stud 50:62–73

Hu, K., Chen, H., Nie, Y., Wang, K., 2015. Seasonal recharge and mean residence times of soil and epikarst water in a small karst catchment of southwest China. Scientific Reports 5

Jia Y, Diao C, Yuan D (2004) The influence of land use on karst water quality of buried karst region-a case of conglin karst ridge-trough at Fuling town. J Nat Resour 19:45–461 **(in Chinese with English abstract)**

Jiang Z, Xia R, Shi J, Pei J, He S, Liang B (2006) The application effects and exploitation capacity of karst underground water resources in southwest China. Acta Geosci Sin 27:495–502 **(in Chinese with English abstract)**

Jiang Y, Zhang C, Yuan D, Zhang G, He R (2008) Impact of land use change on groundwater quality in a typical karst watershed of southwest China: a case study of the Xiaojiang watershed, Yunnan Province. Hydrogeol J 16:727–735

Krimisssa M, Chery L, Fouillac C, Michelot JL (1994) Origin and recharge altitude of the thermo-mineral waters of the eastern Pyrenees. Isot Environ Health Stud 30:317–331

Lan F, Qin X, Jiang Z, Meng R, Mo R, Yang S, Wang W, An S (2015) Influences of Land Use/Land Cover on Hydrogeochemical Indexes of Karst Groundwater in the Dagouhe Basin, Southwest China. Clean Soil Air Water 43:683–689

Lang Y-C, Liu C-Q, Zhao Z-Q, Li S-L, Han G-L (2006) Geochemistry of surface and ground water in Guiyang, China: water/rock interaction and pollution in a karst hydrological system. Appl Geochem 21:887–903

Liu J, Zhao Y, Liu E, Wang D (1997) Discussion on the stable isotope time-space distribution law of China atmospheric precipitation. Site Investigation on Science and Technology, pp 34–39. (in Chinese with English abstract)

Liu W, Wang S, Luo W (2011) The response of epikarst spring to precipitation and its implications in karst peak-cluster region of Libo country, Guizhou Province, China. Geochimica 40:487–496 **(in Chinese with English abstract)**

Liu S, Guo F, Jiang G, Tang Q, Guo X, Huang S (2015) Hydrogeochemical characteristics of peak forest plain in Guilin city, China. Earth Environ 43:55–65 **(in Chinese with English abstract)**

Ma R, Wang Y, Sun Z, Zheng C, Ma T, Prommer H (2011) Geochemical evolution of groundwater in carbonate aquifers in Taiyuan, northern China. Appl Geochem 26:884–897

Pan X, Liang X, Tang J, Su C, Meng X (2015) The patterns and characteristics of four karst groundwater systems in northeast Guizhou slop zone based on the landscape and reservior structure. Acta Geosic Sin 36:85–93 **(in Chinese with English abstract)**

Parkhurst DL, Appelo CAJ (1999) User's guide to PHREEQC (Verstion 2)—a computer program for speciation, batch-reaction, one-dimensional transport, and inverse geochemical calculations. US Geol. Surv. Water-Resour. Inverst. Report, 99-4259

Peng J, Xu YQ, Cai YL, Xiao HL (2011) The role of policies in land use/cover change since the 1970s in ecologically fragile karst areas of Southwest China: a case study on the Maotiaohe watershed. Environ Sci Policy 14:408–418

Pu J (2013) Hydrogen and oxygen isotope geochemistry of karst groundwater in Chongqing. Acta Geosci Sin 34:713–722 **(in Chinese with English abstract)**

Pu T, He Y, Zhang T, Wu J, Zhu G, Chang L (2013) Isotopic and geochemical evolution of ground and river waters in a karst dominated geological setting: a case study from Lijiang basin, South-Asia monsoon region. Appl Geochem 33:199–212

Re V, Sacchi E, Mas-Pla J, Menció A, El Amrani N (2014) Identifying the effects of human pressure on groundwater quality to support water management strategies in coastal regions: a multi-tracer and statistical approach (Bou-Areg region, Morocco). Sci Total Environ 500–501:211–223

Sebela S, Liu H (2014) Structural Geological Characteristics of Karst Caves and Major Stone Forest, Yunnan, China. Acta Carsologica 43:115–127

Thilakerathne A, Schueth C, Chandrajith R (2015) The impact of hydrogeological settings on geochemical evolution of groundwater in karstified limestone aquifer basin in northwest Sri Lanka. Environ Earth Sci 73:8061–8073

Wang Y, Guo Q, Su C, Ma T (2006) Strontium isotope characterization and major ion geochemistry of karst water flow, Shentou, northern China. J Hydrol 328:592–603

Wang H, Jiang X, Wan L, Han G, Guo H (2015a) Hydrogeochemical characterization of groundwater flow systems in the discharge area of a river basin. J Hydrol 527:433–441

Wang L, Li G, Dong Y, Han D, Zhang J (2015b) Using hydrochemical and isotopic data to determine sources of recharge and groundwater evolution in an arid region: a case study in the upper-middle reaches of the Shule River basin, northwestern China. Environ Earth Sci 73:1901–1915

Yang P, Yuan D, Yuan W, Kuang Y, Jia P, He Q (2010) Formations of groundwater hydrogeochemistry in a karst system during storm events as revealed by PCA. Chin Sci Bull 55:788–797 **(in Chinese with English abstract)**

Yang P, Yuan D, Ye X (2013) Sources and migration path of chemical compositions in a karst groundwater system during rainfall events. Chin Sci Bull 58:1755–1763 **(in Chinese with English abstract)**

Yang M, Zhou X, Wang X, Ren Z, Zhang Y, Li X, Shen Y (2015) Characteristics of free carbon dioxide in the hot springs in the Yunlong-Langping area of Yunnan. Hydrogeol Eng Geol 42:156–163 **(in Chinese with English abstract)**

Yuan J (2013) Hydrogeochemistry of the geothermal systems in coastal areas of Guangdong Province, South China. China University of Geosciences, pp 12–130. (in Chinese with English abstract)

Yuan J, Deng G, Xu F, Tang Y, Li P (2016) Hydrogeochemical characteristics of karst groundwater in the northern part of the city of Bijie. Hydrogeol Eng Geol 43:12–21 **(in Chinese with English abstract)**

Zhao Q (1987) The hydrothermal system of Xide geothermal field. J Chengdu Univ Sci Technol 34:123–130 **(in Chinese with English abstract)**

Zhao M, Liu Z, Li H-C, Zeng C, Yang R, Chen B, Yan H (2015) Response of dissolved inorganic carbon (DIC) and δ^{13}CDIC to changes in climate and land cover in SW China karst catchments. Geochim Cosmochim Acta 165:123–136

Zhou P, Qiu Y, Wang C (2015) Analyses of the genesis of Tangshan hot spring area in Nanjing. Geol J China Univ 21:155–162 **(in Chinese with English abstract)**